*31st EPS Conference on Plasma Phys. London, 28 June - 2 July 2004 ECA Vol.**28G**, P-2.194 (2004)*

Physics Results from the National Spherical Torus Experiment

M.G. Bell for the NSTX Research Team

Princeton Plasma Physics Laboratory, Princeton, NJ, U.S.A.

The National Spherical Torus Experiment (NSTX) produces plasmas with aspect ratio A ≡ R/a = 0.85m/0.68m ~ 1.25, at plasma currents up to 1.5 MA with vacuum toroidal magnetic field up to 0.6 T on axis. The plasmas are heated by up to 6 MW of High-Harmonic Fast Waves (HHFW) at a frequency 30 MHz and by 7 MW of deuterium Neutral Beam Injection (NBI) at an energy up to 100 keV. Since January 2004, NSTX has been operating, routinely at toroidal fields up to 0.45 T, with a new central conductor bundle in the toroidal field coil.

Recent experiments have concentrated on optimizing and understanding the beta limits through shaping the plasma cross-section and controlling the plasma profiles. The maximum elongation of the plasma cross section has been increased to $\kappa = 2.6$ and the triangularity (average of upper and lower) to $\delta = 0.8$. This was achieved by improving the feedback control for vertical stability [1] and by employing techniques to broaden the plasma current profile. These techniques include early application of the NBI heating and inducing an early transition to the H-mode by a brief pause in the plasma current ramp. The lower plasma inductance resulting from the high κ and broader current profile has the additional benefit of allowing longer, higher-current pulses within the constraint of the flux swing available from the central solenoid. Toroidal beta up to $\beta_{T,EFIT} = \langle p_{\parallel} + p_{\perp} \rangle / 2 / (B_{T0}^2 / 2\mu_0) = 40\%$ as determined by analysis of the equilibrium with EFIT based external magnetic measurements with the pressure profile shape constrained by the electron pressure $p_e(R)$ measured by Thomson scattering [2]. Figure 1 shows the achieved β_T plotted against normalized plasma current; values of the normalized beta $\beta_N = \beta_T / (I_p / aB_T) = 6.2$ %.m.T/MA have been reached in these low-aspect-ratio plasmas. The gains in normalized current from the higher κ and δ achieved in recent operation are evident. Analysis of the profile data with the TRANSP code [3] yields $\beta_{T,TRANSP} = \langle p_{\parallel} + 2p_{\perp} \rangle / 3 / (B_{T0}^2 / 2\mu_0) = 34\%$ using a classical Monte-Carlo model for the thermalization of the energetic ions from NBI. The waveforms of the shot with highest β_T are shown in Fig. 2 and the profiles of T_i, T_e, n_e and v_i, the toroidal ion velocity, and a cross-section of the plasma equilibrium at the time of maximum β_T are shown in Fig. 3. Note that the very high ion toroidal rotation velocity relative to the Alfvén velocity, $v_i/v_A \sim 0.3$, affects the

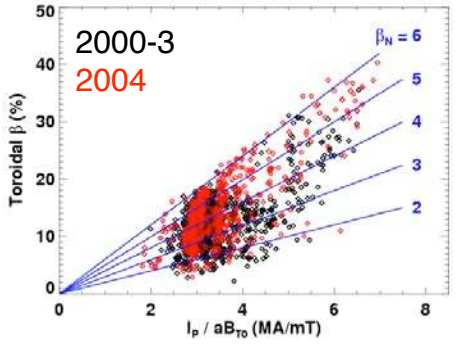

Fig. 1 Toroidal beta from EFIT vs. Troyon-normalized plasma current.

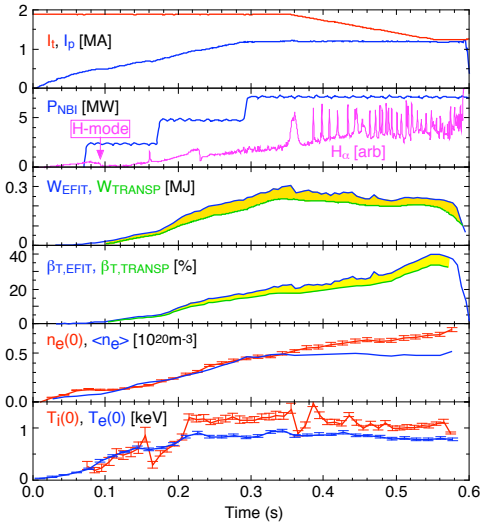

Fig. 2 Waveforms for the NSTX shot achieving the highest β_T.

equilibrium significantly, leading to an outward shift of the density profile with respect to the flux surfaces [4]. This lower-single-null divertor discharge was initiated at higher toroidal magnetic field to achieve the most quiescent current ramp phase before reducing the field to achieve the highest β_T. The mechanisms responsible for the beta limit in different operating conditions are discussed in [5] and the effects of MHD on fast-ion confinement in [6].

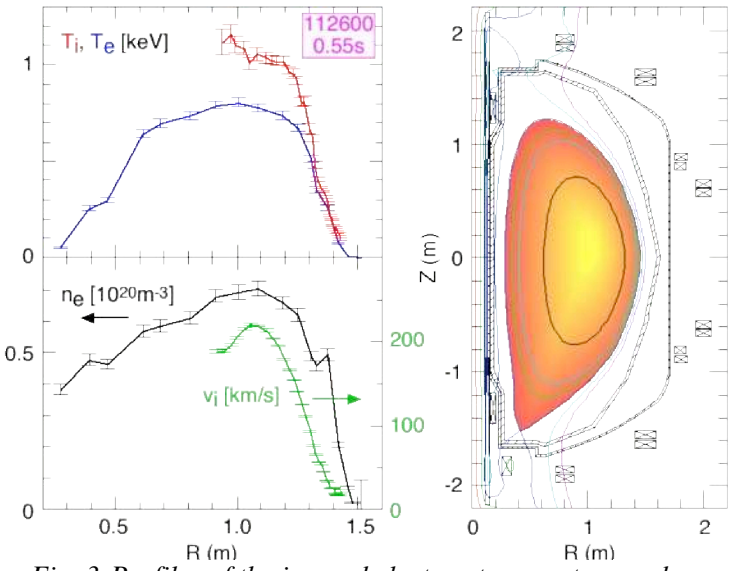

Fig. 3 Profiles of the ion and electron temperature and ion toroidal velocity and electron density at peak β_T.

Boronization is applied in NSTX, at intervals of 1 day to 2 weeks, to control impurities [7] and helium glow discharge cleaning is performed between plasma shots to remove deuterium from plasma-facing surfaces. In addition, prior to the highest β shot, an ohmically heated helium discharge had been run to reduce the recycling further and control the edge density which otherwise can rise rapidly following the H-mode transition. To improve the gas fueling efficiency, a supersonic gas injection nozzle, capable of injecting a collimated jet at ~1.5 km/s at the outside midplane is being installed on NSTX [8].

The basic dependences of the total and thermal confinement time in NSTX on plasma current and NBI heating power are similar to those of conventional tokamaks, both in controlled single-parameter scans and in regression fits to the NSTX database. This is shown in Fig. 4, where a dependence of the total confinement time from the EFIT magnetic analysis, $\tau_E \propto I_p^{0.84\pm0.05} P_{tot}^{-0.49\pm0.04}$ is inferred for H-mode discharges spanning the ranges $0.6 \le I_p[MA] \le 1.2$, $1.5 \le P_{NB}[MW] \le 7$. However, the total confinement times exceed the ITER-97L [9] scaling for confinement by factors 1.5 – 2.5 for discharges both with and without H-mode transitions. It is particularly encouraging that enhancements of the

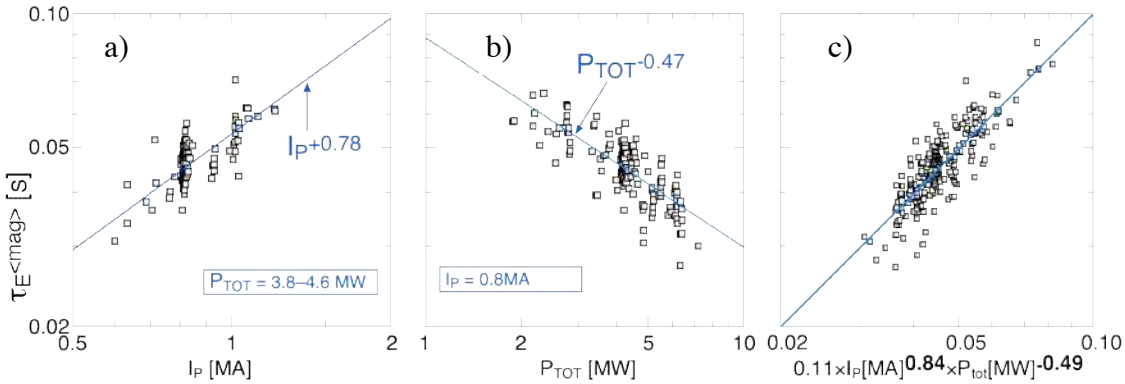

Fig. 4 Fits to the magnetically determined energy confinement time for H-mode deuterium discharges with B_T = 0.45 T, κ = 1.8 – 2.4 at the time of peak total electron energy. a) $\tau_E \propto I_p^{+0.78}$ at constant P_{tot}, b) $\tau_E \propto P_{tot}^{-0.47}$ at constant I_p, c) Regression to both I_p, P_{tot}.

confinement over ITER-97L scaling by a factor $H_{97L} = 2$ have been maintained as the density was raised by gas puffing to the Greenwald limit. The thermal confinement times have been analyzed by TRANSP for a smaller dataset to date, but in H-mode plasmas these too exceed the corresponding ITER-98Hpb(y,2) scaling.

The TRANSP analysis shows that the dominant thermal loss is through the electron channel in both H- and L- mode plasmas. This situation is consistent with gyro-kinetic calculations of the plasma stability [10] which show that the ion temperature gradient modes may be stabilized by the large shear in the toroidal rotation. Figure 5 shows the measured profiles and the thermal diffusivities for the ions and electrons calculated by TRANSP for a low-density L-mode discharge which shows evidence for an internal transport barrier, *i.e.* a region of reduced χ_e and χ_i, near r/a ≈ 0.5. Although this shot did not show an H-mode transition, its confinement was enhanced over L-mode by a factor $H_{97L} \approx 2.4$. The relationship between this transport reduction and possible reversal of the magnetic shear,

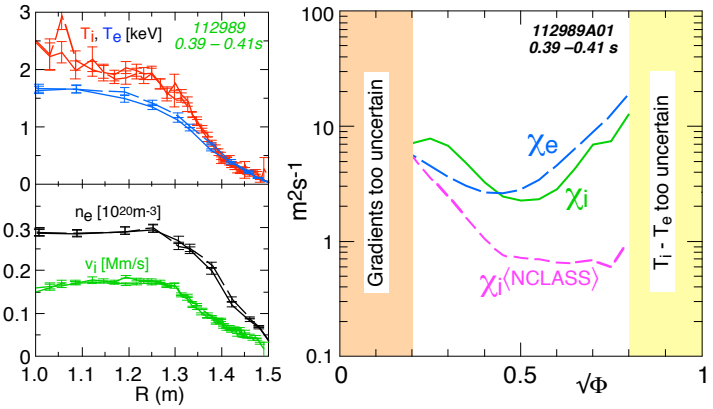

Fig. 5 a) Profiles of the ion and electron temperature, ion toroidal velocity and electron density and b) profiles of the ion and electron and neoclassical ion thermal diffusivities for a low-density L-mode plasma with an apparent internal transport barrier.

will be investigated using the motional-Stark-effect diagnostic which is now being commissioned on NSTX. In some high-density ($n_e(0) \sim 8 \times 10^{19} m^{-3}$) NBI-heated, H-mode plasmas, recent analyses [11] of the power balance taking account of the experimental uncertainties have confirmed that the ion thermal diffusivity drops to the neoclassical level, or even below in some cases.

Significant electron heating has been produced by HHFW power in low-density deuterium and helium plasmas. The most effective heating has been observed when the toroidal array of 12 poloidal coupling straps has been phased to launch waves with a symmetrical toroidal wavenumber spectrum peaked at $k_{tor} \approx \pm 14\ m^{-1}$ or $\pm 7\ m^{-1}$. The HHFW heating can induce H-mode transitions in deuterium plasmas and, as with NBI, there is a striking buildup of the density in the edge following the H-mode transition. However, the overall confinement in the plasmas heated by HHFW is lower than for NBI heating. Figure 6 shows the measured plasma total and the electron energy and the prediction based on ITER-97L scaling assuming that all the launched RF power is coupled to the

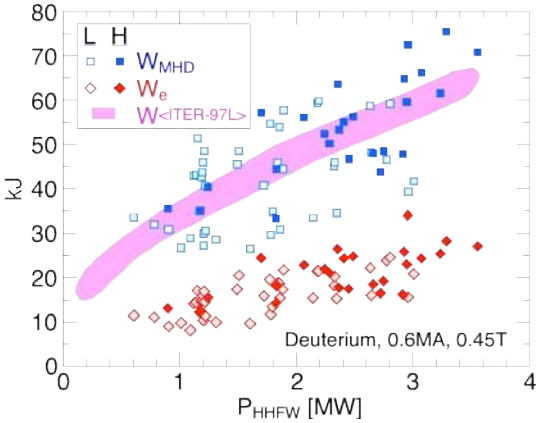

Fig. 6 Measured total and electron energies in deuterium plasmas heated by HHFW.

plasma. The H-mode cases tend to exceed the L-mode plasmas in total and electron energy but the central electron temperatures in the H-mode actually tend to be lower, suggesting that less power is deposited in the center with H-mode profiles. The HHFW frequency is about 9 times the deuteron cyclotron frequency at the plasma axis, so little direct absorption of the waves by the thermal ions is expected in NSTX, although an interaction of the HHFW with the energetic ions from NBI has been previously observed and explained [12]. Experiments are underway to determine whether the difference in the effect on the plasma between the HHFW and the NBI heating is caused by the difference in the division of the heating power between the electrons and ions, or whether there are additional absorption or loss mechanisms at work with HHFW heating. A spectrometer measuring helium emission from the plasma edge has revealed the development of a substantial hot ion population, with perpendicular temperatures up to ~0.5 keV, during HHFW heating [13]. Evidence has also been obtained from a Langmuir probe with high frequency response inserted into the far scrape-off layer, for a possible parametric decay of the launched waves into ion Bernstein waves at harmonics of the local deuteron cyclotron frequency. When the HHFW coupler array was phased to produce co- and counter- directed waves with $k_{tor} \approx \pm (3.5 - 7)\ m^{-1}$ in pairs of otherwise matched plasmas, differences were measured in the toroidal loop voltage (corrected for inductive effects), indicating current drive estimated to be about 100 kA [14].

In H-mode plasmas, a variety of ELM activity occurs; examples are seen in the D_α light trace in Fig. 2. After a quiescent phase following the H-mode transition, small frequent ELMs occur between 0.25 and 0.35 s. These ELMs have characteristics different from other well-known types and have tentatively been designated as “Type V” [15]. The large (Type I) ELMs which begin at about 0.35 s become more frequent as the toroidal field is reduced, whereas in a companion shot with constant toroidal field, they remained sporadic.

The presenting author wishes to thank colleagues in the NSTX research team for providing data and for helpful discussion of these results. This work is supported by U.S. DOE Contract DE-AC02-76CH03073.

References

[1] D. Mueller *et al.*, *paper P2-199, this conference.*
[2] S.A. Sabbagh *et al.*, Phys. Plasmas **9** (2002) 2085
[3] J. Ongena *et al.*, Fusion Technology **33** (1997) 181
[4] J. Menard, Nucl. Fusion **43** (2003) 330.
[5] A.C. Sontag *et al.*, *paper P2-193, this conference.*
[6] S.S. Medley *et al.*, *paper P2-200, this conference.*
[7] H.W Kugel *et al.*, J. Nucl. Mater. **313–316** (2003) 187
[8] V. Soukhanovskii *et al.*, *paper P2-190, this conference.*
[9] ITER Physics Expert Groups, Nuclear Fusion **39** (1999) 2175
[10] M. Redi *et al.*, *paper P2-162, this conference.*
[11] B.P. LeBlanc *et al.* Nuclear Fusion **44** (2004) 513.
[12] A.L. Rosenberg *et al.*, Physics of Plasmas, **11** (2004) 2441-2452.
[13] T.M. Biewer *et al.*, *paper P2-198, this conference.*
[14] J.R. Wilson, Phys. Plasmas **10** (2003) 1733
[15] R. Maingi *et al.*, *submitted to J. Nucl. Mater., May 2004 and paper P2-189, this conference.*